Supporting Information

Østby et al. 10.1073/pnas.1210627109

SI Materials and Methods

Sample. A total of 164 children and adolescents aged 9–22 were recruited through newspaper advertisements, local schools, and workplaces as part of an ongoing longitudinal study at the Center for the Study of Human Cognition at the Department of Psychology, University of Oslo (for details, see refs. 1–3). The study was approved by the Regional Ethical Committee of South Norway. Written informed consent was obtained from all participants older than 12 y of age and from a parent/guardian of volunteers under 16 y of age. Oral informed consent was obtained from all participants under 12 y of age. Participants had no self or parent-reported history of neurological or psychiatric disorders, chronic illness, premature birth, learning disabilities, or use of medicines known to affect nervous system functioning. They were further required to be right-handed, speak Norwegian fluently and have normal or corrected to normal hearing and vision. Among the initial 164 children and adolescents who met the inclusion criteria, time or tiredness prevented a subset of participants to complete the remembering–imagination task (see below). Of the 107 who completed the task, 4 had no useable T1-weighted MRI scans, reducing the final sample to 103 for structural analyses (female, $n = 52$; age, 9.1–21.9 y; mean, 16.4; SD, 3.4). All participants scored 85 or above on full-scale IQ (mean, 111; SD, 10; range, 85–136) (4). There was no significant effect of sex ($t[101] = -0.37$; $P = 0.71$) or age on IQ ($r = 0.17$; $P = 0.08$) or of sex on age ($t = 0.26$; $P = 0.79$). Of these 103, 10 did not have usable BOLD scans, reducing the sample to 93 for the functional connectivity analyses.

Cue-Word Task. The task was modeled on a much-used cue-word paradigm for probing past and future events (5) (Table S1). The task was to remember past experiences and envision possible future scenarios in response to cue words within 2 y into the past/future. The participants were asked to retrieve/imagine specific episodes that could happen, within a time frame of minutes to hours (no longer than a day), to imagine episodes that they thought might actually happen to them, and to not recast exact memories as future scenarios. A practice trial and six tasks was administered. A cue word was presented on a computer screen together with a word designating either "past" or "future" by use of E-prime software. The participants were then asked to think of an episode that the cue word reminded them of and to press a key when they had found a relevant episode. They were then given 40 s to think through the episode and imagine it in as much detail as they could.

The six cue words were chosen to be neutral-positive, easy to relate to, and open to many possible scenarios. The assignment of a cue word to each of the two conditions was fixed and equal for all participants, and the cue words were pairs of thematically similar words, divided between the two conditions. They were presented in Norwegian in the following order: "bursdag" (birthday-past), "ferie" (vacation/holiday-future), "skog" (forest-past), "feiring" (celebration-future), "reise" (travel-past), "sjø" (sea-future). The emotional valence and intensity of English translations of four of the words (from both conditions) were checked against the Affective Norms for English Words (ANEW) (6), and all four fell within the positive affect range of the scale (7.12–8.16) and had an emotional arousal value ranging from 4.95 to 6.68. The words "celebration" and "forest" were not found in the ANEW, but were considered of similar to the equivalents "birthday" and "sea."

Each past and future episode was immediately rated by the participants on a one-page questionnaire, asking about the participant's experience during the act of remembering/imagining. The questionnaire consisted of 11 items (see below). Some of the items were sampled from the Memory Experiences Questionnaire (7), whereas others were modified or new, made for the purposes of the present study. The questions regarded the phenomenological experience of the episodes, rated on a five-point Likert scale (strongly disagree to strongly agree). The questionnaire yielded a total phenomenology (autonoetic) score (mean of all items), as well as a perspective score (items 6 and reversed 8), experiential score (items 2, 5, 9, and 11), and coherence score (items reversed 3, reversed 7, 10).

Interitem reliability was tested using Cronbach's α. For past, Cronbach's α was 0.67, 0.70, and 0.59 for each of the three cue words, whereas corresponding numbers for future were 0.69, 0.73, and 0.70. Thus, primary scores of interest were autonoetic past, which was the mean score of all questions related to the three cue words to which the participants were asked to recall an episode, and autonoetic future, which was the mean score in response to the cue-words to which a future episode was imagined.

The questionnaire was answered immediately after each cue-word task. The questionnaire was presented in Norwegian, in language adjusted to fit the age range of the participants in the study. We have not attempted to adjust the English translation in the same way. Items that are reversed during scoring are marked with an R.

MRI Scanning and Analyses. Each MP-RAGE was visually inspected, and the scan with the highest quality was used for the analyses. All datasets were processed and analyzed at the Neuroimaging Analysis Lab, Center for the Study of Human Cognition, University of Oslo. T1-weighted scans were analyzed with FreeSurfer 5.1 (http://surfer.nmr.mgh.harvard.edu/fswiki), yielding continuous measures of area vertex-wise across the cortical mantle, as well as ICV and hippocampal volume. Hippocampus was estimated based on an automated segmentation procedure (8) that assigns a neuroanatomical label to each voxel in an MR volume based on probabilistic information automatically estimated from a manually labeled training set (8, 9). ICV was estimated by use of an atlas-based normalization procedure (10). Surface area maps of the gray matter–white matter boundary were computed for each subject by calculating the area of every triangle in a cortical surface tessellation. The triangular area at each point in native space are compared with the area of the analogous points in registered space to give an estimate of surface area expansion or contraction continuously along the cortical surface (11, 12). Maps were smoothed using a circularly symmetric Gaussian kernel across the surface with a full width at half-maximum (FWHM) of 20 mm and averaged across participants using a nonrigid high-dimensional spherical averaging method to align cortical folding patterns (13). This procedure provides accurate matching of morphologically homologous cortical locations among participants on the basis of each individual's anatomy while minimizing metric distortion, resulting in a measure of cortical area for each person at each point on the reconstructed surface.

Resting-state fMRI analysis of the 100 volumes in time were carried out using Multivariate Exploratory Linear Optimized Decomposition into Independent Components (MELODIC) (14) implemented in FSL (15, 16) (www.fmrib.ox.ac.uk/fsl). Individual processing included discarding the first three volumes to let the scanner reach equilibrium because of progressive saturation, motion correction, spatial smoothing using a Gaussian kernel of full-width at half-maximum (FWHM) of 6 mm, and high-pass temporal filtering equivalent to 150 s.

FMRI volumes were registered to the subjects' T1-weighted skull stripped using FreeSurfer (17) by means of FMRIB's Linear Image Registration Tool (FLIRT) (18, 19). The linear alignment was optimized using a version of FLIRT that has implemented a boundary-based approach similar to Greve and Fischl (20). The T1-weighted volume was warped to Montreal Neurological Institute-152 standard space (MNI-152) using FMRIB's Nonlinear Image Registration Tool (FNIRT) (21, 22), and the resulting nonlinear transform was applied to the FMRI data. Next, the processed functional datasets were temporally concatenated across subjects to create a single 4D data set and submitted to group independent component analysis (ICA) using MELODIC.

The between-subject analysis was carried out using dual regression (23, 24), allowing for voxel-wise analysis of resting functional connectivity. This specific method has been proven more consistent and reliable than template-matching approaches in its ability to estimate individual-level resting state networks from group-level (g)ICA spatial maps (25). The procedure comprises three steps. First, group-wise spatial ICA is applied to the temporally concatenated resting-state FMRI data. Here, dimensionality estimation was performed by using the Laplace approximation to the Bayesian evidence for a probabilistic principal component (26, 27), resulting in 20 group IC spatial maps.

Second, the dual-regression algorithm (23, 24, 28) is applied to identify subject-specific time courses and spatial maps. Here, a set of gICA spatial maps is used in a linear model fit against the individual FMRI dataset. This results in matrices reflecting the temporal dynamics of the corresponding RSN for each of the 191 subjects. These time-course matrices are then normalized by their variance and used in a linear model fit against the individual FMRI data set. This temporal regression yields subject-specific spatial maps reflecting degree of synchronization, reflecting both amplitude and coherence across space (29, 30). Here, the full set of 20 gICA maps reflecting various RSNs and artifact components were included in the dual regression.

Third, the individual functional connectivity maps are collected across subjects into one 4D file per component, with the fourth dimension being subject identification, and submitted to voxel-wise cross-subject statistics. All gIC maps are shown in Fig. S1. Component number 10 (outlined in the white box) showed high connectivity values in the precuneus/posterior cingulate/retrosplenial cortex, as well as the medial prefrontal cortex. This corresponded very well to the posterior default-mode network. No other component showed this pattern of connectivity. Other gICs corresponded either to nonresting-state artifacts or activation of less interest for the present study and were, thus, not included in further analyses. One possible exception to this was IC 1, which could resemble a more anterior part of the DMN. Our a priori hypothesis was that a relationship existed between connectivity of the posterior default-mode network and score on the cue-word task, based on previous research establishing that the posterior default-mode network (precuneus, posterior cingulate) is involved in pro- and retrospective memory processes. Thus, only the gIC reflecting the posterior default-mode network was included in the final cross-subject statistics. This had the additional benefit of minimizing the number of statistical tests performed. However, because IC 1 showed some overlap with the anterior DMN, a post hoc exploratory analysis was performed for this component also.

An ICA approach was chosen because data acquired with resting fMRI does not easily lend itself to standard GLM analysis (31). In our opinion, an ICA statistical approach is the best available for identification of resting-state networks. ICA-based identified resting-state networks have been shown to have high test–retest reliability (32) and significant heritability (33) and to be sensitive biomarkers for psychiatric and neurodegenerative diseases (34, 35).

Noise and artifacts, e.g., from head movement and cardiac and respiratory pulsations, pose inherent problems in analyses of fMRI data. Even when various preprocessing steps are used to remove such effects, some residual noise is likely. By use of ICA, we know that the component reflecting the posterior DMN is statistically independent of other components. Previous studies have shown that approaches like ICA can separate certain sources of noise, such as respiratory depth, from the signal of interest (36, 37). Important sources of noise may be picked up in separate components, not reflecting relevant neuronal activity. ICA may be a more powerful approach than conventional regression-based techniques to identify real activations of interest distinguished from noise inherent in all fMRI data.

Recently, it has been demonstrated that in-scanner head motion may substantially impact MRI measurements of resting-state functional connectivity (38, 39), and this is especially important to control for in studies of development, where the amount of motion is likely to vary as a function of age. This problem may be somewhat reduced by the use of ICA, because sources of nonresting-state–related activations may be separated out from the component of interest (40). Kiviniemi et al. (41) showed that BOLD signal sources representing resting-state networks was separated from artifact sources by use of ICA, including motion (26). In addition, we assessed motion by calculating mean relative volume-to-volume displacement, which summarizes total volume-to-volume translation and rotation across all three axes. In the current sample, motion was, as expected, negatively correlated with age ($r = -0.34$; $P < 0.001$). Additional analyses were, thus, performed to test whether motion affected the results, by including estimated motion as an additional nuisance covariate in the partial correlation analyses.

Comparing BOLD activation across a wide age range may also be problematic because of challenges attributable to normalization of activation to the same template if brain size varies systematically with age. To assess this, we correlated age with total brain volume and found a low, not significant, correlation ($r = -0.12$, $P = 0.239$). Furthermore, we correlated total brain volume with the functional connectivity values from the cluster significantly related to past autonoetic score and found that these were not related ($r = 0.022$; $P = 0.836$). Thus, we believe that it is unlikely that developmental differences in brain size unduly have affected the connectivity analyses.

SI Results

Area and connectivity showed negative age correlations. For area, these did not survive corrections for multiple comparisons, and so the uncorrected results threshold at $P < 0.05$ are shown as background information (Fig. S2). For rBOLD, the corrected results are shown. As can be seen, the age relationships do not overlap much with the default-mode component.

1. Ostby Y, et al. (2009) Heterogeneity in subcortical brain development: A structural magnetic resonance imaging study of brain maturation from 8 to 30 years. *J Neurosci* 29:11772–11782.
2. Tamnes CK, et al. (2010) Neuroanatomical correlates of executive functions in children and adolescents: A magnetic resonance imaging (MRI) study of cortical thickness. *Neuropsychologia* 48:2496–2508.
3. Tamnes CK, et al. (2010) Brain maturation in adolescence and young adulthood: Regional age-related changes in cortical thickness and white matter volume and microstructure. *Cereb Cortex* 20:534–548.
4. Wechsler D (1999) *Wechsler Abbreviated Scale of Intelligence* (The Psychological Corp., San Antonio, TX).
5. Schacter DL, Addis DR, Buckner RL (2007) Remembering the past to imagine the future: The prospective brain. *Nat Rev Neurosci* 8:657–661.
6. Bradley MM, Lang PJ (1999) *Affective Norms for English Words (ANEW): Instruction Manual and Affective Ratings. Technical Report C-1* (Center for Research in Psychophysiology, Univ. of Florida, Gainesville, FL).
7. Sutin AR, Robins RW (2007) Phenomenology of autobiographical memories: The memory experiences questionnaire. *Memory* 15:390–411.

8. Fischl B, et al. (2002) Whole brain segmentation: Automated labeling of neuroanatomical structures in the human brain. *Neuron* 33:341–355.
9. Fischl B, et al. (2004) Sequence-independent segmentation of magnetic resonance images. *Neuroimage* 23(Suppl 1):S69–S84.
10. Buckner RL, et al. (2004) A unified approach for morphometric and functional data analysis in young, old, and demented adults using automated atlas-based head size normalization: Reliability and validation against manual measurement of total intracranial volume. *Neuroimage* 23:724–738.
11. Fischl B, Sereno MI, Dale AM (1999) Cortical surface-based analysis. II: Inflation, flattening, and a surface-based coordinate system. *Neuroimage* 9:195–207.
12. Dale AM, Fischl B, Sereno MI (1999) Cortical surface-based analysis. I. Segmentation and surface reconstruction. *Neuroimage* 9:179–194.
13. Fischl B, Sereno MI, Tootell RB, Dale AM (1999) High-resolution intersubject averaging and a coordinate system for the cortical surface. *Hum Brain Mapp* 8:272–284.
14. Beckmann CF, DeLuca M, Devlin JT, Smith SM (2005) Investigations into resting-state connectivity using independent component analysis. *Philos Trans R Soc Lond B Biol Sci* 360:1001–1013.
15. Smith SM, et al. (2004) Advances in functional and structural MR image analysis and implementation as FSL. *Neuroimage* 23(Suppl 1):S208–S219.
16. Woolrich MW, et al. (2009) Bayesian analysis of neuroimaging data in FSL. *Neuroimage* 45(1 Suppl):S173–S186.
17. Ségonne F, et al. (2004) A hybrid approach to the skull stripping problem in MRI. *Neuroimage* 22:1060–1075.
18. Jenkinson M, Smith S (2001) A global optimisation method for robust affine registration of brain images. *Med Image Anal* 5:143–156.
19. Jenkinson M, Bannister P, Brady M, Smith S (2002) Improved optimization for the robust and accurate linear registration and motion correction of brain images. *Neuroimage* 17:825–841.
20. Greve DN, Fischl B (2009) Accurate and robust brain image alignment using boundary-based registration. *Neuroimage* 48:63–72.
21. Andersson JLR, Jenkinson M, Smith S (2007) Non-linear optimisation. *FMRIB Technical Report TR07JA1*. Available at www.fmrib.ox.ac.uk/analysis/techrep. Accessed February 1, 2012.
22. Andersson JLR, Jenkinson M, Smith S (2007) Non-linear registration, aka spatial normalisation. *FMRIB Technical Report TR07JA2*. Available at www.fmrib.ox.ac.uk/analysis/techrep. Accessed February 1, 2012.
23. Beckmann CF, Mackay CE, Filippini N, Smith SM (2009) Group comparison of resting-state FMRI data using multi-subject ICA and dual regression. *Neuroimage* 47 (Supplement 1):S39–S41.
24. Filippini N, et al. (2009) Distinct patterns of brain activity in young carriers of the APOE-epsilon4 allele. *Proc Natl Acad Sci USA* 106:7209–7214.
25. Zuo XN, et al. (2010) Reliable intrinsic connectivity networks: Test-retest evaluation using ICA and dual regression approach. *Neuroimage* 49:2163–2177.
26. Beckmann CF, Smith SM (2004) Probabilistic independent component analysis for functional magnetic resonance imaging. *IEEE Trans Med Imaging* 23:137–152.
27. Minka TP (2000) Automatic choice of dimensionality for PCA. *MIT Media Laboratory Perceptual Computing Section Technical Report No. 514* (MIT Media Laboratory, Vision and Modeling Group, Cambridge, MA).
28. Cole DM, Smith SM, Beckmann CF (2010) Advances and pitfalls in the analysis and interpretation of resting-state FMRI data. *Front Syst Neurosci* 4:8.
29. Roosendaal SD, et al. (2010) Resting state networks change in clinically isolated syndrome. *Brain* 133:1612–1621.
30. Cole DM, et al. (2011) Orbitofrontal connectivity with resting-state networks is associated with midbrain dopamine D3 receptor availability. *Cereb Cortex*, 10.1093/cercor/bhr354.
31. Beckmann CF (2012) Modelling with independent components. *Neuroimage* 62: 891–901.
32. Zuo XN, et al. (2010) The oscillating brain: Complex and reliable. *Neuroimage* 49: 1432–1445.
33. Glahn DC, et al. (2010) Genetic control over the resting brain. *Proc Natl Acad Sci USA* 107:1223–1228.
34. Calhoun VD, Eichele T, Pearlson G (2009) Functional brain networks in schizophrenia: A review. *Front Hum Neurosci* 3:17.
35. Greicius MD, Srivastava G, Reiss AL, Menon V (2004) Default-mode network activity distinguishes Alzheimer's disease from healthy aging: Evidence from functional MRI. *Proc Natl Acad Sci USA* 101:4637–4642.
36. Beckmann CF, DeLuca M, Devlin JT, Smith SM (2005) Investigations into resting-state connectivity using independent component analysis. *Philos Trans R Soc Lond B Biol Sci* 360:1001–1013.
37. Fukunaga M, et al. (2006) Large-amplitude, spatially correlated fluctuations in BOLD fMRI signals during extended rest and early sleep stages. *Magn Reson Imaging* 24: 979–992.
38. Van Dijk KR, Sabuncu MR, Buckner RL (2011) The influence of head motion on intrinsic functional connectivity MRI. *Neuroimage* 59:431–438.
39. Satterthwaite TD, et al. (2012) Impact of in-scanner head motion on multiple measures of functional connectivity: relevance for studies of neurodevelopment in youth. *Neuroimage* 60:623–632.
40. Calhoun VD, Liu J, Adali T (2009) A review of group ICA for fMRI data and ICA for joint inference of imaging, genetic, and ERP data. *Neuroimage* 45(1 Suppl):S163–S172.
41. Kiviniemi V, et al. (2009) Functional segmentation of the brain cortex using high model order group PICA. *Hum Brain Mapp* 30:3865–3886.

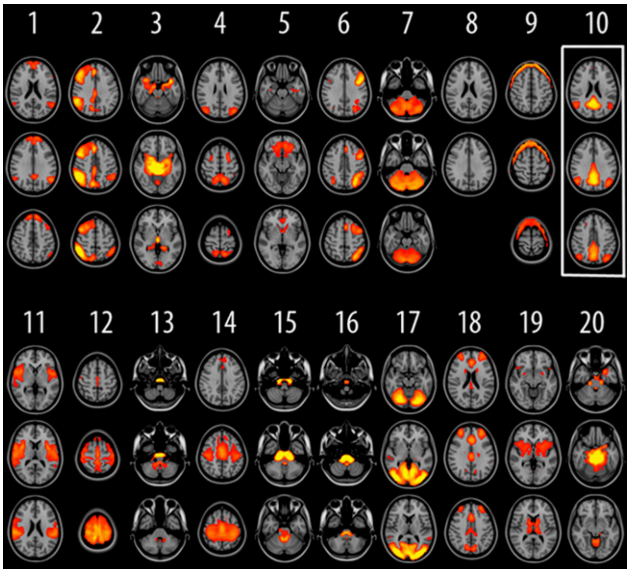

Fig. S1. Results of the 20-component ICA solution. The 10th component was regarded as the one best representing the posterior default-mode network.

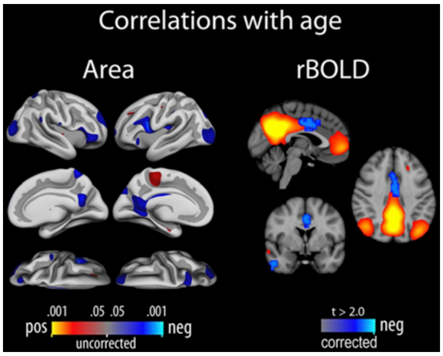

Fig. S2. Correlations between age and local cortical arealization (*Left)* and functional connectivity (*Right*).

Table S1. Rating scale for past and future episodes

It was difficult for me to think of this event. (R)	1	2	3	4	5
I remembered/thought of sounds.	1	2	3	4	5
This experience came to me in bits and pieces, not as a coherent story. (R)	1	2	3	4	5
I recognized the setting in which it took place.	1	2	3	4	5
It was almost like being there.	1	2	3	4	5
I saw the event through my own eyes.	1	2	3	4	5
The event was a blending of many similar, related events. (R)	1	2	3	4	5
I viewed this as if I was an observer to the event. (R)	1	2	3	4	5
I saw a lot, for instance faces, thing, colors.	1	2	3	4	5
The order of happenings within the event was clear.	1	2	3	4	5
I had a lot of sensory experiences (sounds, smells, tastes, etc.).	1	2	3	4	5
This event was easy for me to think of.	1	2	3	4	5

1, disagree; 2, partly disagree; 3, neither agree nor disagree; 4, partly agree; 5, agree. Items that are reversed during scoring are marked with (R).